Available online at www.sciencedirect.com

ScienceDirect

Advances in Space Research 53 (2014) 1290–1303

ADVANCES IN SPACE RESEARCH (a COSPAR publication)

www.elsevier.com/locate/asr

TEC derived from some GPS stations in Nigeria and comparison with the IRI and NeQuick models

A.B. Rabiu [a,b,*], A.O. Adewale [c], R.B. Abdulrahim [a,d], E.O. Oyeyemi [c]

[a] National Space Research and Development Agency (NASRDA), Abuja, Nigeria
[b] Space Physics Laboratory, Federal University of Technology, Akure, Nigeria
[c] University of Lagos, Lagos, Nigeria
[d] Centre for Satellite Technology, NASRDA, Abuja, Nigeria

Received 31 October 2013; received in revised form 1 February 2014; accepted 6 February 2014
Available online 15 February 2014

Abstract

Total electron content (TEC) measured simultaneously using Global Positioning System (GPS) ionospheric monitors installed at some locations in Nigeria during the year 2011 ($Rz = 55.7$) was used to study the diurnal, seasonal, and annual TEC variations. The TEC exhibits daytime maximum, seasonal variation and semiannual variations. Measured TEC were compared with those predicted by the improved versions of the International Reference Ionosphere (IRI) and NeQuick models. The models followed the diurnal and seasonal variation patterns of the observed values of TEC. However, IRI model produced better estimates of TEC than NeQuick at all locations.

Keywords: Ionosphere; GPS; Total electron content; IRI; NeQuick

1. Introduction

Total electron content (TEC) is the number of electrons present per m^2 along a pathway between two points. It is the integral of electron density along the ray path between ground stations and Global Positioning System (GPS) satellites, with units of electrons per square meter, where 10^{16} electrons/$m^2 = 1$ TEC unit (TECU) (Bhuyan and Borah, 2007). Maximum TEC usually occurs in the early afternoon and minimum TEC usually occurs just before sunrise over Nigeria (Adewale et al., 2011, 2012).

The GPS is a satellite-based navigation system consisting of a network of 24 satellites in 6 orbital planes with 4 satellites in each plane. The GPS satellites orbit at an altitude of about 20,200 km with an orbital plane inclination of 55° to the Earth's equator. Each satellite transmits signals at two frequencies, 1575.42 MHz (L1) and 1227.60 MHz (L2). GPS provides accurate position, velocity and time information globally and continuously under all weather conditions. The system has three segments:

(i) The Space Segment
(ii) The Control Segment, and
(iii) The User Segment (the GPS receivers).

The Space Segment consists of the 24 GPS satellites. The Control Segment consists of four monitor stations and four ground antennas which are distributed around the Earth, and a master control station located in Colorado Springs, USA. The User Segment consists of both military and civilian GPS receivers (Kintner and Ledvina, 2005; Misra and Enge, 2006).

* Corresponding author at: National Space Research and Development Agency (NASRDA), Abuja, Nigeria. Tel.: +234 8030705787.
E-mail address: tunderabiu2@gmail.com (A.B. Rabiu).

http://dx.doi.org/10.1016/j.asr.2014.02.009
0273-1177/

The equatorial ionosphere exhibits many unique features in electron density and temperature, such as the plasma fountain, equatorial electrojet, the equatorial ionization anomaly (EIA). These features are caused by the horizontal orientation of the geomagnetic field lines at the equator and the shift between the geographic and geomagnetic equator (Bhuyan and Borah, 2007). EIA is the redistribution of ionization densities, with a depression (or trough) at the geomagnetic equator and two peaks (crests) on either side of the equator, at about 15° magnetic latitudes (Appleton, 1946). According to Mitra (1946), the depression exists because plasma produced by photo ionization at higher altitudes over the magnetic equator diffuses downwards and outwards to the north and south of the magnetic equator, and leaving depletion at the equator. The strength of the equatorial electrojet (EEJ) also affects plasma distribution in the equatorial ionosphere. This is as a result of the coupling between E and F region electric fields (Fejer et al., 1981).

Bhuyan and Borah (2007) studied the diurnal, seasonal and latitudinal variation of TEC derived from GPS network in India during 2003–2004. The TEC exhibits features like the equatorial noon time bite-out, annual and semiannual variations, the equatorial ionization anomaly, and day-to-day variability. Their result showed that daytime variability is less at and near the equator than at the crest of the anomaly, whereas nighttime variability is high compared to the daytime variability in all seasons and at all latitudes of the India sector. The time of occurrence of the diurnal maximum in TEC also varies with season. In the work of Obrou et al. (2009), TEC over Korhogo (9.33°N, 5.43°W) decrease gradually from 0000 h to 0600 h local time (LT) where it reaches a minimum value and it has an increasing variation that is linear in the time range from 0600 h to 1100 h LT and gradual after 1100 h LT until 1800 h LT. After sunset, TEC decreases until mid-night. Considering the seasonal variation, TEC values exhibit a peak value of 35 TECU in December solstice and a peak value of 25 TECU in June Solstice.

Several authors have investigated the performance of International Reference Ionosphere (IRI) and NeQuick models in predicting TEC at different locations (Migoya Orué et al., 2008; Coïsson et al., 2008; Bidaine and Warnant, 2010; Adewale et al., 2011, 2012; Okoh et al., 2012). Okoh et al. (2012) worked with data recorded at Nsukka (6.87°N, 7.38°E; dip latitude −2.97°), a single location in Nigeria, and concluded that the IRI TEC values generally compared well with the GPS observed TEC values with correlation coefficients as good as about 0.9, and root-mean square deviations generally around 20–50% for diurnal comparisons. Earlier, Adewale et al. (2011), using data from Lagos (6.5°N, 3.4°E; dip latitude 3.03°S), reported that IRI-2007 (NeQuick option) gave a relatively poor TEC prediction between 0200 h and 0600 h LT, with the TEC percentage deviation (ΔTEC) having values greater than 50% during all seasons considered in year 2009. The ΔTEC never exceeded 50% at any other hour of the day except at 0800 h LT during both December solstice and September equinox. The NeQuick option was run from IRI web interface (http://ccmc.gsfc.nasa.gov/modelweb/models/iri_vitmo.php) and the upper boundary of electron density profile in the IRI model was specified as 2000 km and B0 Table option for bottomside electron density shape parameter was used. A newer version of NeQuick model is now available that can integrate the electron density profile to an altitude of 20,000 km, hence it is important to validate this new version of NeQuick. Similarly, a newer version of IRI model (IRI-2011) is available.

This present work seeks to investigate the transient variations of TEC obtained from measurement at six stations in Nigeria and compared the results with those derived from the improved versions of the IRI and NeQuick models for the locations. The result of this study will show the potential of the European NeQuick model and the IRI models at predicting TEC values over Nigeria.

2. Data and method

The GPS data, for the year 2011, used for TEC variability and validation of IRI2011 and NeQuick models, were obtained courtesy of the Office of the Surveyor General of the Federal Government of Nigeria, which is the mapping agency of Nigeria. Starting from 2008 the mapping agency installed a network of state-of-the art GPS Continuous Operating Reference Stations (CORS), primarily for geodetic purpose (Jatau et al., 2010). The GPS network is termed NIGNET (NIGerian GNSS Reference NETwork). The GPS data is in Receiver Independent Exchange (RINEX) format. RINEX is data interchange format for raw satellite navigation system data. The coordinates of the six stations used for this study are given in Table 1. Fig. 1 shows a map of Nigeria indicating the location of the GPS receivers and the magnetic equator over Nigeria.

The RINEX observation files were processed by the GPS-TEC analysis application software, developed by Gopi Seemala of the Institute for Scientific Research, Boston College, USA.

The ionosphere is a dispersive medium, hence the GPS frequencies L1 (1575.42 MHz) and L2 (1227.6 MHz)

Table 1
Coordinates of GPS receiver locations.

Station code	Location	Geographical coordinates		Geomagnetic coordinates	
		Latitude (°N)	Longitude (°E)	Latitude (°)	Longitude (°E)
RUST	Port Harcourt	4.80	6.98	−4.33	78.76
UNEC	Enugu	6.42	7.50	−3.25	79.36
ULAG	Lagos	6.52	3.40	−3.03	75.45
FUTY	Yola	9.35	12.50	−1.32	84.31
CGGT	Bauchi	10.12	9.11	−0.96	81.09
BKFP	Birnin-Kebbi	12.47	4.23	0.72	76.62

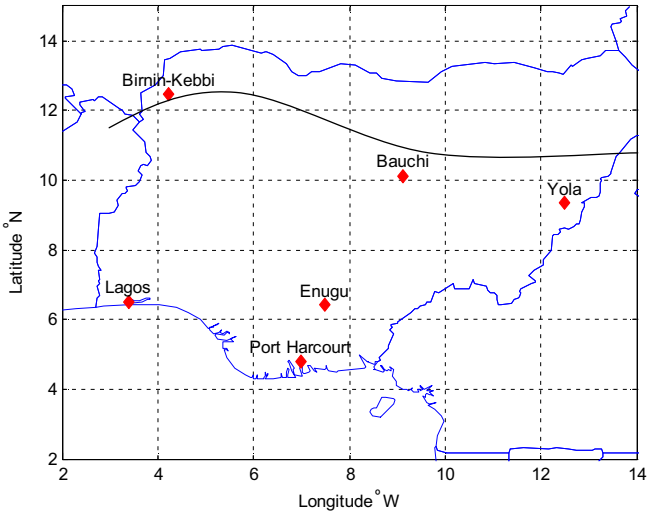

Fig. 1. Map of Nigeria showing the geographical locations of the GPS receiver stations used in this study and the magnetic equator.

experience different group delays and phase advances. TEC from group delay, using pseudo-range measurements, is given by

$$\mathrm{TEC}_{group} = \frac{1}{40.3}\left(\frac{1}{f_1^2} - \frac{1}{f_2^2}\right)^{-1}(P_1 - P_2) \quad (1)$$

where f_1 and f_2 are L1 and L2 carrier frequencies, and P_1 and P_2 are pseudo-range observables.

TEC from carrier phase measurements is given by

$$\mathrm{TEC}_{phase} = (C_1 - C_2) \times 2.852 \quad (2)$$

where C_1, C_2 are C/A and L2C code measurements.

Calculation of TEC from group delay measurement is absolute and noisy. The relative phase delay between the two carrier frequencies gives a more precise measure of relative TEC, but is ambiguous because the actual number of cycles of phase is unknown. The ambiguity term is resolved by combining the two estimates of TEC (Eqs. (1) and (2)) to form an improved estimate of absolute TEC (Warnant and Pottiaux, 2000).

The GPS-TEC software calculates VTEC from the observation data using a suitable mapping function. The mapping function $S(E)$ is given by (Mannucci et al., 1993)

$$S(E) = \frac{1}{\cos z} = \left\{1 - \left(\frac{R_E \times \cos(E)}{R_E + h_S}\right)^2\right\}^{-0.5} \quad (3)$$

where

z = zenith angle of the satellite as seen from the observing station,
R_E = radius of the Earth,
E = the elevation angle in radians, and
h_s = the altitude of the thin layer above the surface of the Earth (taken as 350 km).

In order to minimize the multipath effects on GPS data for variability and validation study, an elevation angle cut off of 30° was used. In addition to eliminating the errors from multipath, the satellite and receiver biases were removed from the TEC values used in this present study. The satellite and receiver bias values were obtained from the data centre of Bern University, Switzerland.

We have used VTEC values for March Equinox (MAREQUI) (February, March, April), June Solstice (JUNSOLS) (May, June, July), September Equinox (SEPEQUI) (August, September, October), and December Solstice (DECSOLS) (November, December, January), for the year 2011, with an average sunspot number (R) of 55.7 to represent a period of medium solar activity (MSA). The observed monthly sunspot numbers for 2011 is shown in Table 2.

The observed values of VTEC are compared with the values modelled by the IRI-2011 and NeQuick models. Both IRI and NeQuick models are used for predicting ionospheric electron density. IRI is an empirical ionospheric model based on experimental observations of the ionospheric plasma. The IRI model describes monthly averages of the electron density, electron temperature, ion composition, ion temperature, and ion drift in the current altitude range of 50–2000 km. The accuracy of the IRI model in a specific region and/or time period depends on the availability of reliable data for the specific region and time since it is a data-based model (Bilitza and Reinisch, 2008). Daily TEC values from IRI-2011 model were obtained from a MATLAB script written by Dr. Patrick Sibanda and Dr. Pierre Cilliers of South African National Space Agency (SANSA). The online model is available at http://ccmc.gsfc.nasa.gov/modelweb/models/iri_vitmo.php. We selected 2000 km as the upper boundary of electron density profiles and the B0 Table option for the bottomside electron density shape parameter.

However, the NeQuick model is based on the Di Giovanni–Radicella (DGR) model (Di Giovanni and Radicella, 1990) which was modified to give vertical electron content from ground to 1000 km consistent with the European Cooperation in the field of Scientific and

Table 2
Observed monthly sunspot numbers.

Month	Sunspot number
January	19.0
February	29.4
March	56.2
April	54.4
May	41.6
June	37.0
July	43.9
August	50.6
September	78.0
October	88.0
November	96.7
December	73.0

Technical Research (COST) 238 regional electron content model (Radicella and Zhang, 1995). NeQuick is a "profiler" which makes use of three profile anchor points, namely the E layer peak (at a fixed height of 120 km), F1 peak, and F2 peak. It uses the ionosonde parameters foE, foF1, foF2 (critical frequencies) and M3000(F2) (propagation factor) to model the anchor points. The bottom side of the electron density profile consists of the superposition of three Epstein layers, which peak at the anchor points. The Epstein layers have different thickness parameters for their bottom and topsides (5 "semi-Epstein" layers). The topside of the electron density profile consists of the topside of an Epstein layer with a height dependent thickness parameter (Coïsson et al., 2006; Nava et al., 2008). The NeQuick source code package used for this study uses the following inputs: height (km), latitude (degrees N), longitude (degrees E), month (1...12), 10.7 cm solar radio flux (flux units) and Universal Time (hours). The output (function value) is daily vertical total electron content (VTEC) in TEC units (TECU) and the selected upper boundary for the electron density is 2000 km.

We have used all the available days of the month in 2011 for the observed and predicted averages in all the stations.

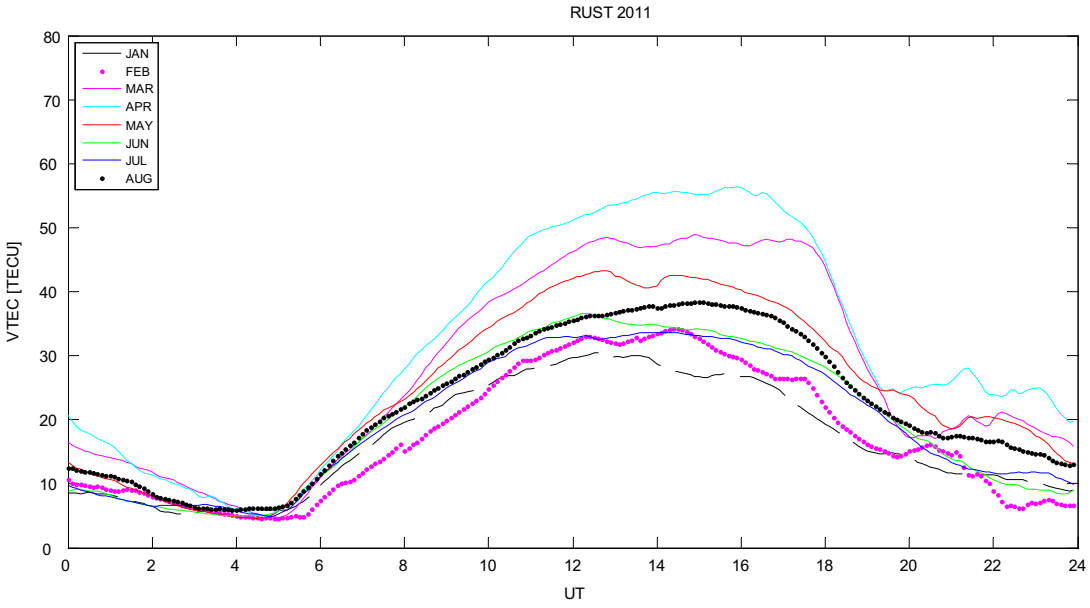

Fig. 2. Monthly mean VTEC for RUST.

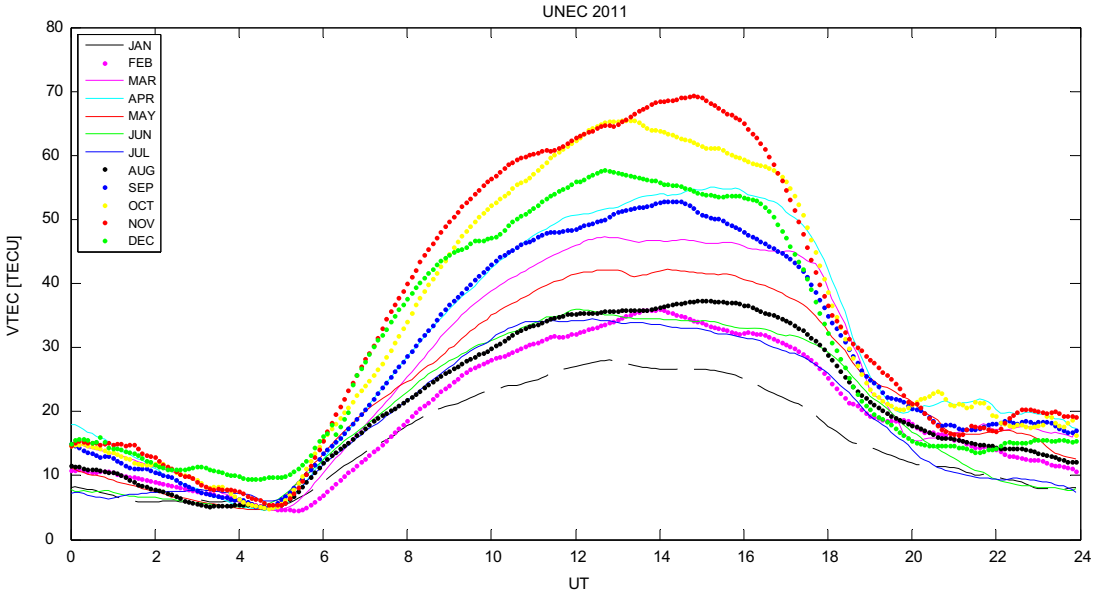

Fig. 3. Monthly mean VTEC for UNEC.

The root-mean-square error (*RMSE*) has been used to quantify the performance of the models;

$$RMSE = \sqrt{\sum_{i=1}^{N} \frac{1}{N} (VTEC_{obs} - VTEC_{mod})^2} \quad (4)$$

$$RMSE_{average} = \frac{1}{N} \sum_{i=1}^{N} (RMSE)_i \quad (5)$$

where N is the number of data points and $VTEC_{obs}$ and $VTEC_{mod}$ are the observed and modelled VTEC values, respectively.

3. Results and discussion

Figs. 2–7 show the average monthly plots of VTEC diurnal variations for all the stations with the exception of December in CGGT and September, October, November and December in RUST due to instrument failure. RUST, UNEC, ULAG and FUTY are located very close to the magnetic equator; between the crest of the southern equatorial anomaly and the equator. CGGT and BKFP are located on the magnetic equator. The plot shows that VTEC has higher values during daytime compared with nighttime values, over all the stations and in all the months.

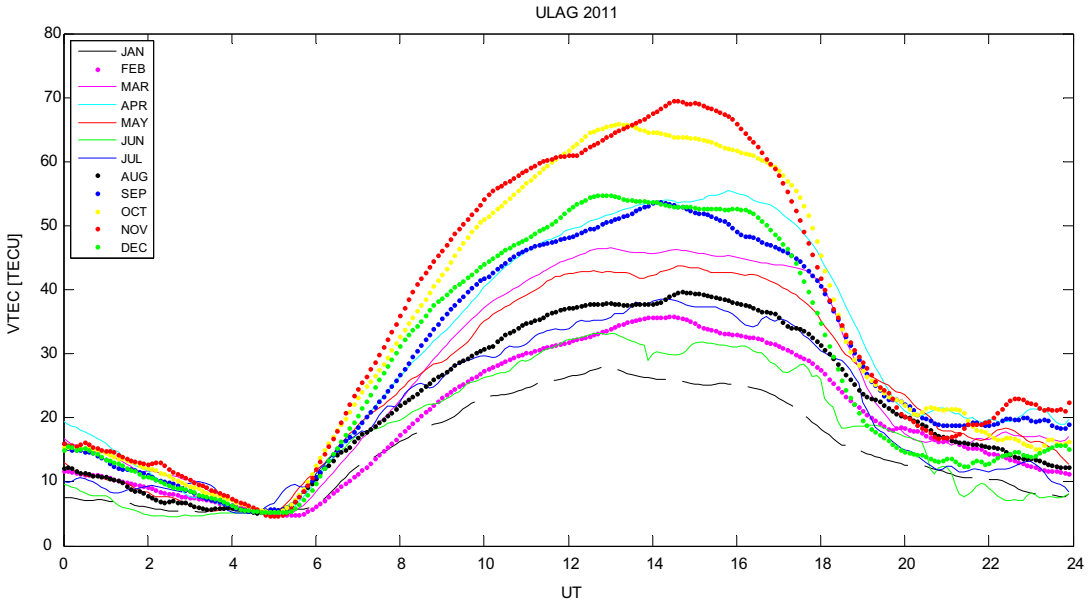

Fig. 4. Monthly mean VTEC for ULAG.

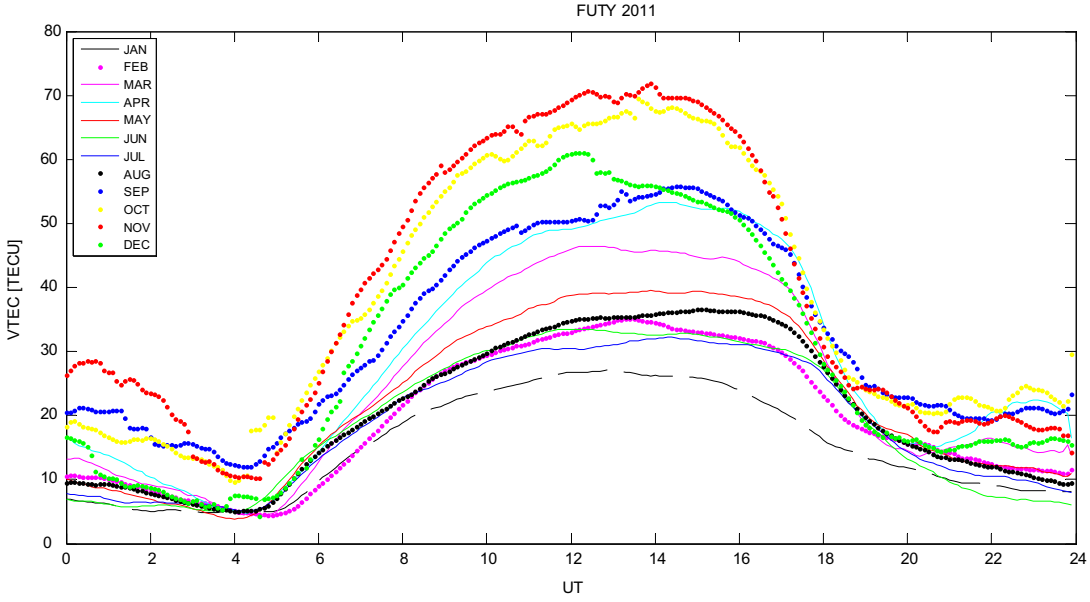

Fig. 5. Monthly mean VTEC for FUTY.

(Figs. 9–12) VTEC values generally increase from 0600 LT for all the months and reach a maximum value during 1500–1700 LT. In addition, VTEC exhibits the usual diurnal variation of a minimum in the pre-sunrise hours (0600 LT) at all the stations and months. These diurnal variations are caused by Extreme Ultraviolet flux, geomagnetic activity, equatorial electrojet and local atmospheric conditions in the thermosphere (Bagiya et al., 2009). Observations at the different Nigerian stations showed that the VTEC values are high in November, followed by October and December. VTEC values are low in January, compared to the other months. Ideally, during the daytime, the equator is hotter than the North and South poles. This causes meridional wind flows towards the poles from the equator. As reported by Balan et al. (2000) and Bagiya et al. (2009), this flow of meridional wind changes the neutral composition and O/N_2 decreases at equatorial stations. This decrease in O/N_2 ratio, which is maximum during the equinox months, will result in higher electron density. Hence equinox VTEC will be highest. However, our result shows that VTEC is highest in November, a solstice month. The explanation for this observation is as a result of the dramatic variation of solar activity in the year 2011. The sunspot number in November of year 2011 was more than

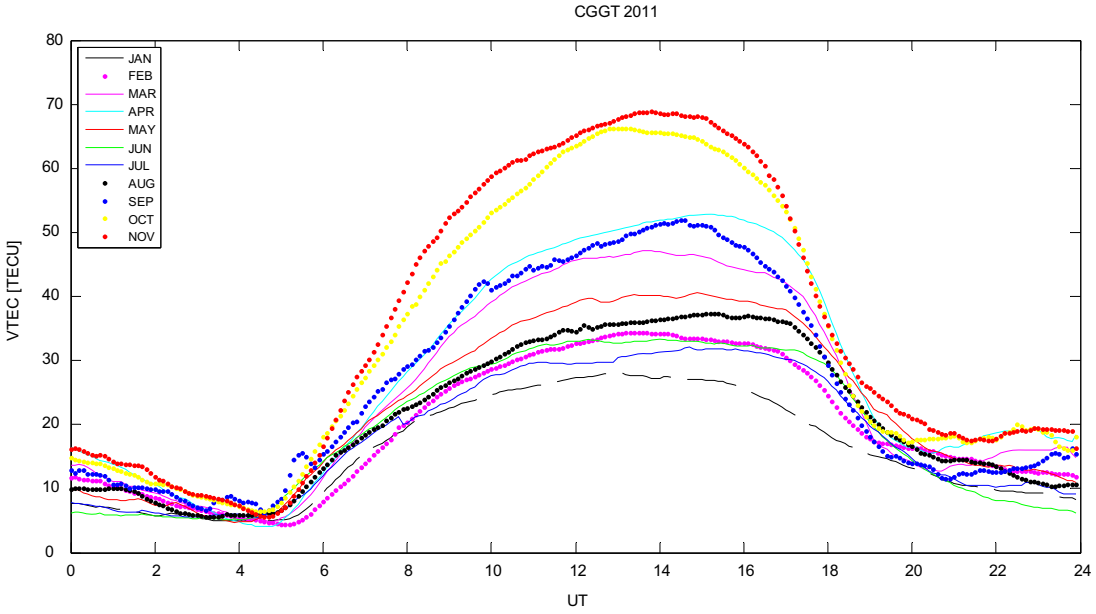

Fig. 6. Monthly mean VTEC for CGGT.

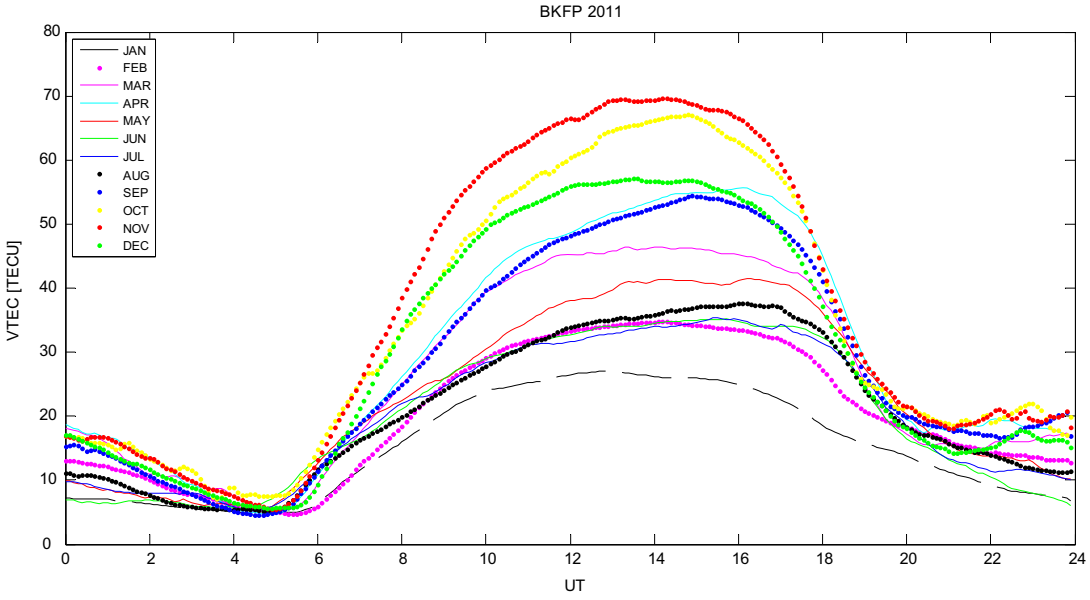

Fig. 7. Monthly mean VTEC for BKFP.

that of the other month and the sunspot in January is the lowest, as shown in Table 2. This is likely responsible for the offset of the normal seasonal pattern of the year under consideration. The VTEC values for January and November (both are months in DECSOLS) show remarkable differences. The peak values of VTEC in all the stations vary from about 20–30 TECU and 68–72 TECU, in January and November respectively. This large difference in VTEC values between the peak values in January and November is because of the large difference between the sunspot

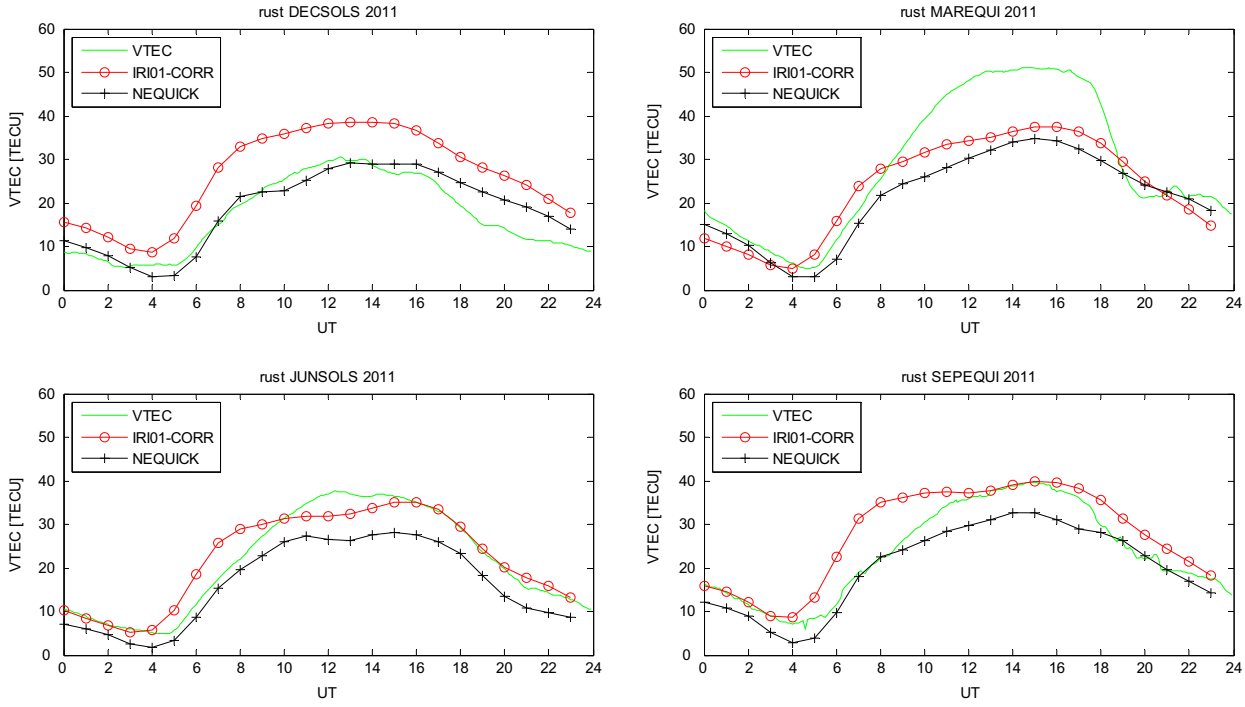

Fig. 8. Diurnal variations of observed mean values of TEC at RUST along with the IRI and NeQuick predicted values.

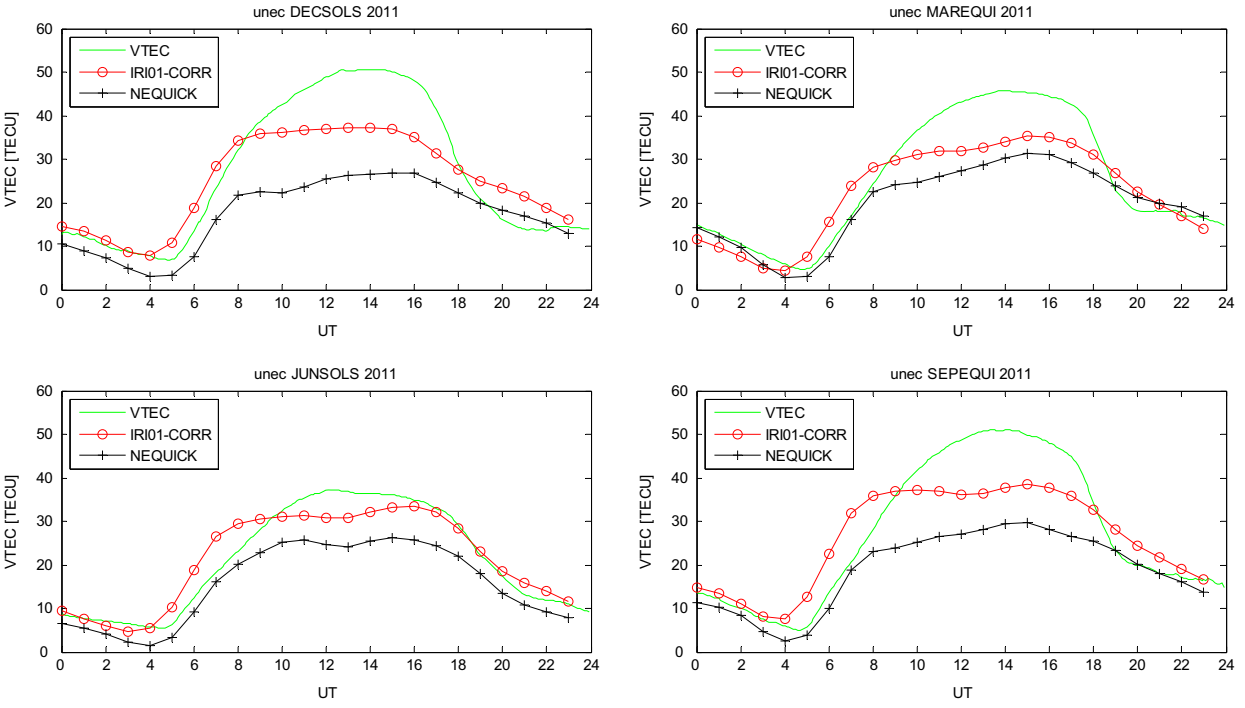

Fig. 9. Diurnal variations of observed mean values of TEC at UNEC along with the IRI and NeQuick predicted values.

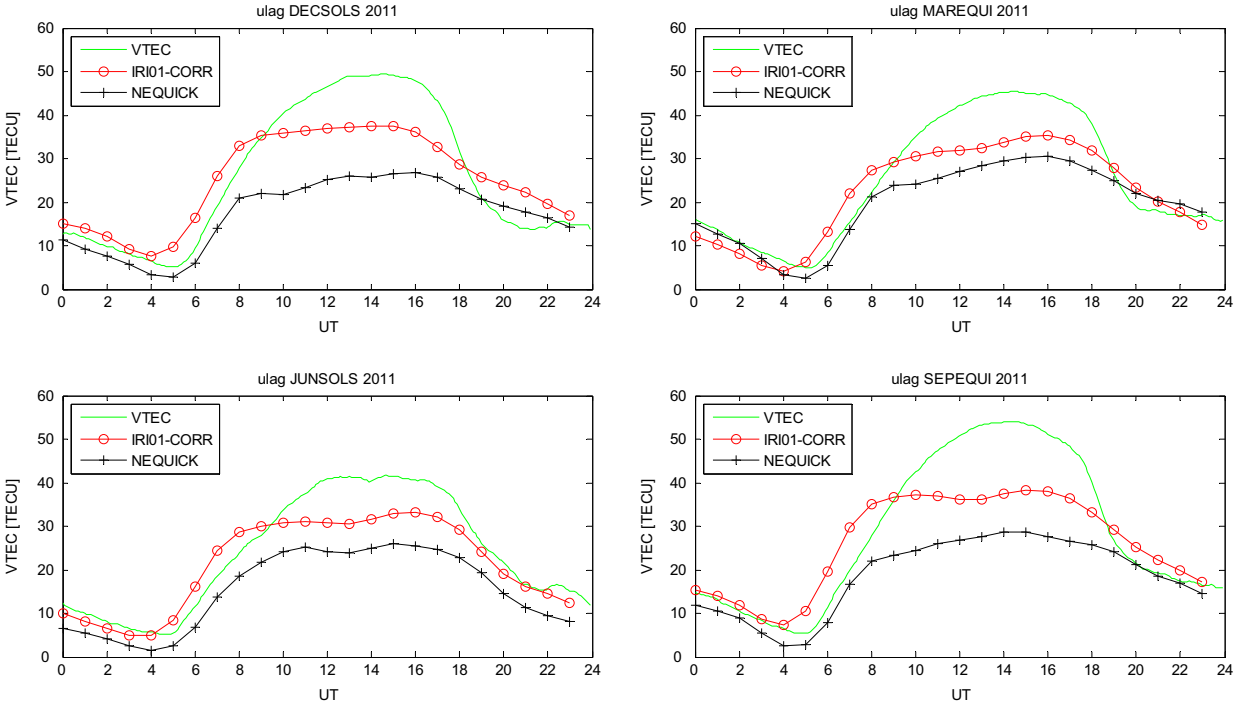

Fig. 10. Diurnal variations of observed mean values of TEC at ULAG along with the IRI and NeQuick predicted values.

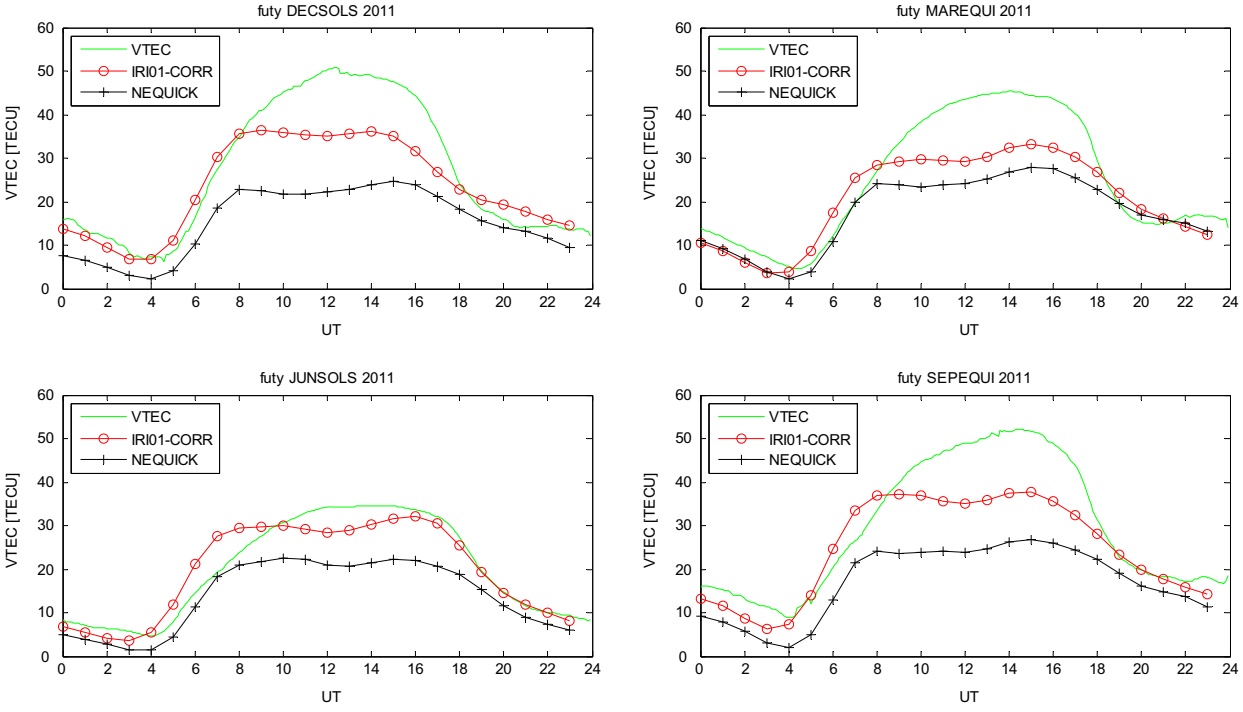

Fig. 11. Diurnal variations of observed mean values of TEC at FUTY along with the IRI and NeQuick predicted values.

number for January and November. Generally, the crest of the diurnal maximum is higher in equinoxes and lower in JUNSOLS, thus exhibiting the semiannual variation.

The comparisons of experimental VTEC with predicted VTEC are shown in Figs. 8–13. Each figure shows the diurnal and seasonal comparisons for the stations. In all the stations the predictions are relatively good during the night period. However, during the daytime the models show an under estimation in all the seasons and at all the stations except during DECSOLS at RUST which showed an over estimation for IRI. The IRI plot is closer to the observed VTEC during the daytime, at all the stations and all

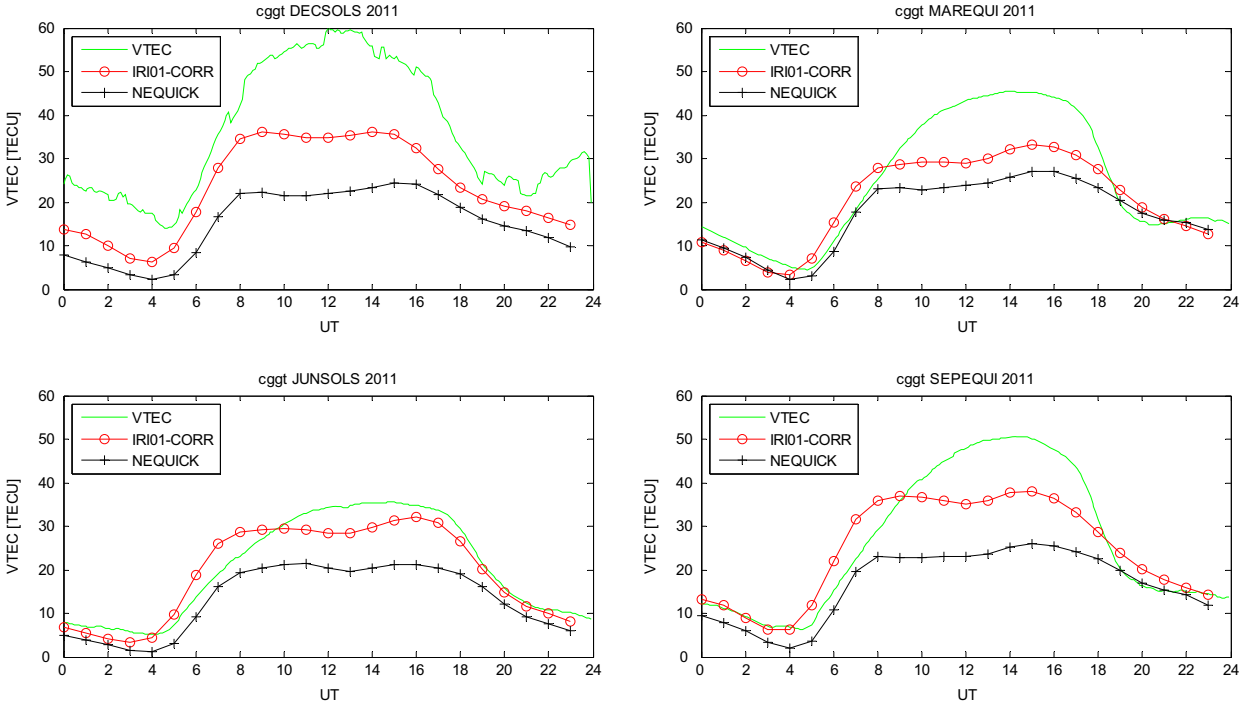

Fig. 12. Diurnal variations of observed mean values of TEC at CGGT along with the IRI and NeQuick predicted values.

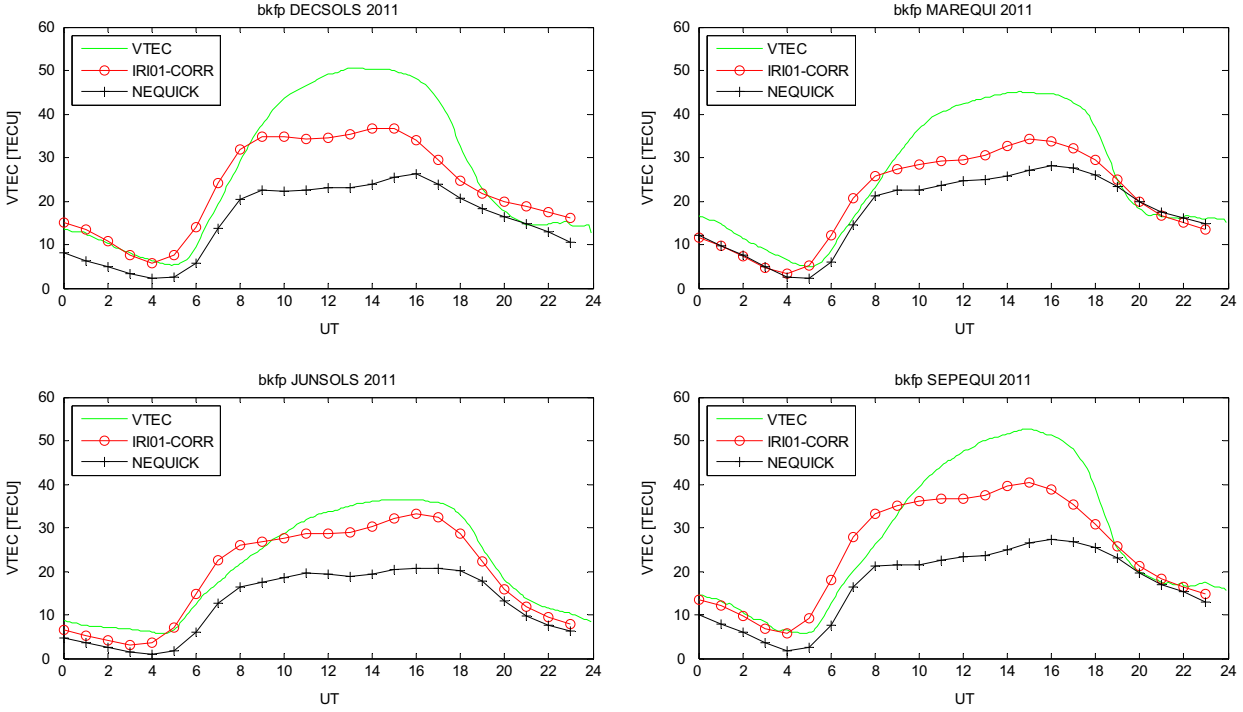

Fig. 13. Diurnal variations of observed mean values of TEC at BKFP along with the IRI and NeQuick predicted values.

seasons. The models showed the noon bite out which is not shown in the observed VTEC. This feature shows the predicted VTEC decreasing by 5 TECU around 1400 LT in almost all the stations and seasons for a short time and then recovers. In the work of Aggarwal (2011), the observed VTEC in Indian sector shows the noontime bite out around 1400 LT in November and December months. The noon bite out was also observed by Mukherjee et al. (2010) during equinox month season in Indian EIA region.

The differences between the observed VTEC and predicted VTEC are shown in Figs. 14–19. The plots showed that the prediction is worst during daytime, most especially

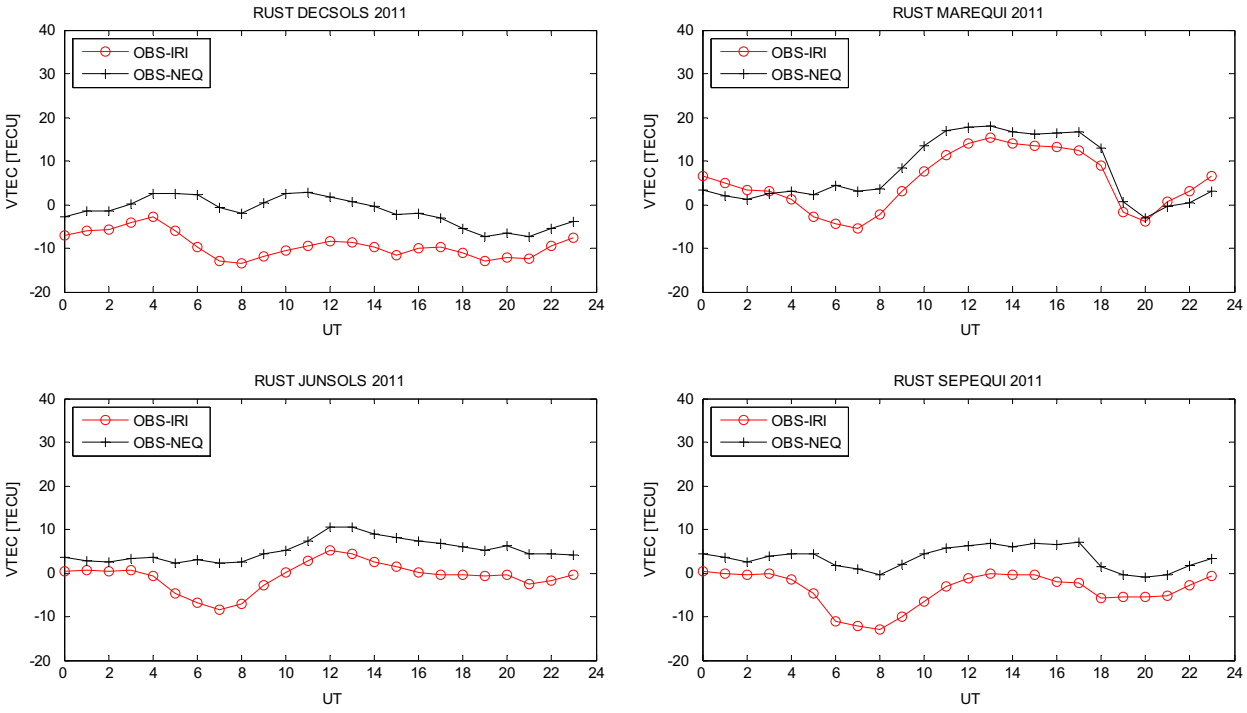

Fig. 14. Plots of $\Delta(VTEC_{OBS} - VTEC_{PRE})$ for RUST.

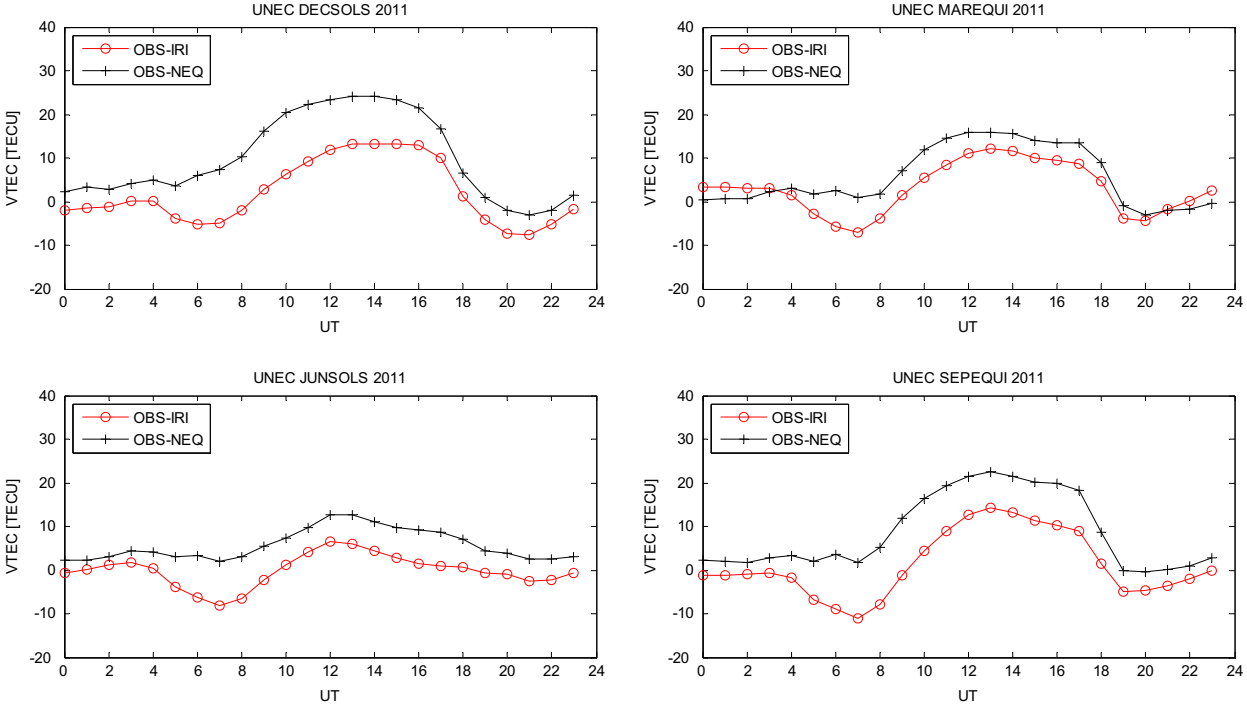

Fig. 15. Plots of $\Delta(VTEC_{OBS} - VTEC_{PRE})$ for UNEC.

during DECSOLS for NeQuick model. The difference between experimental VTEC and predicted VTEC can be attributed to the plasmaspheric content. The experimental GPS-VTEC was calculated along the propagation path of a satellite-emitted signal from an altitude of 20,200 km over the Earth to the GPS receivers; however, the upper boundary for the predicted VTEC is 2000 km. Gulyaeva and Gallagher (2007) reported that the plasmaspheric contribution to the GPS-VTEC could vary from 10% during daytime under quiet magnetic conditions to more than

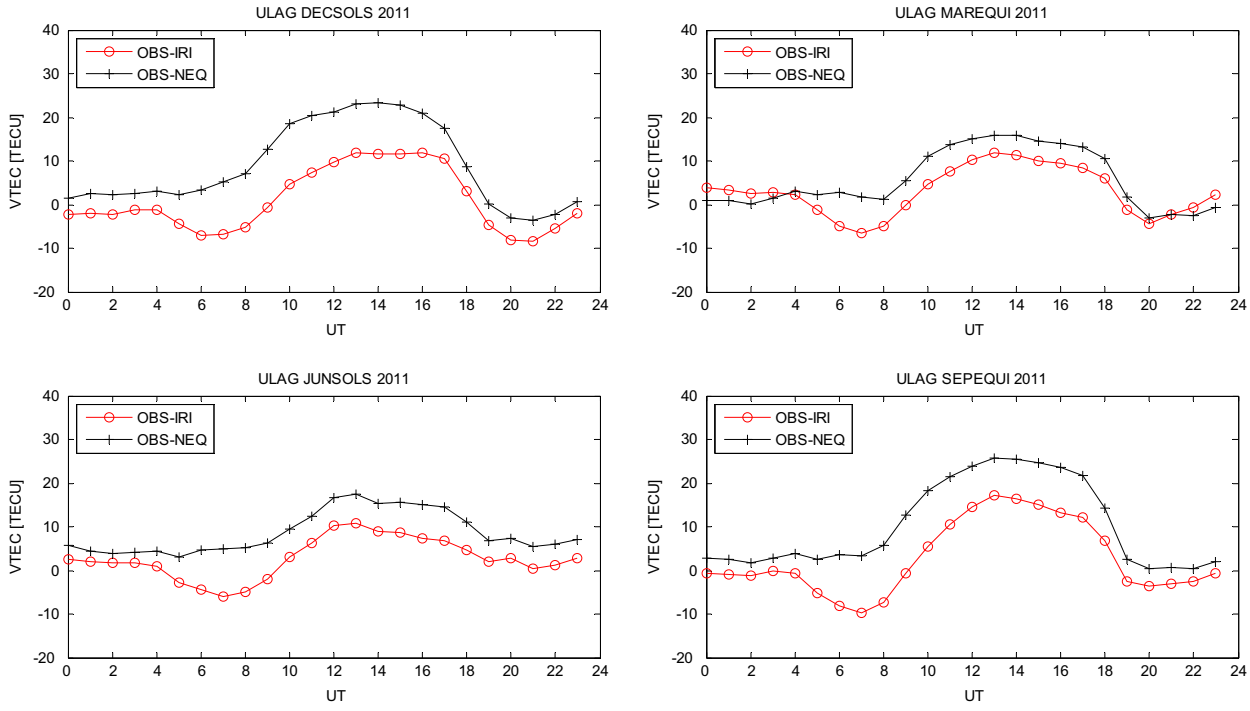

Fig. 16. Plots of $\Delta(VTEC_{OBS} - VTEC_{PRE})$ for ULAG.

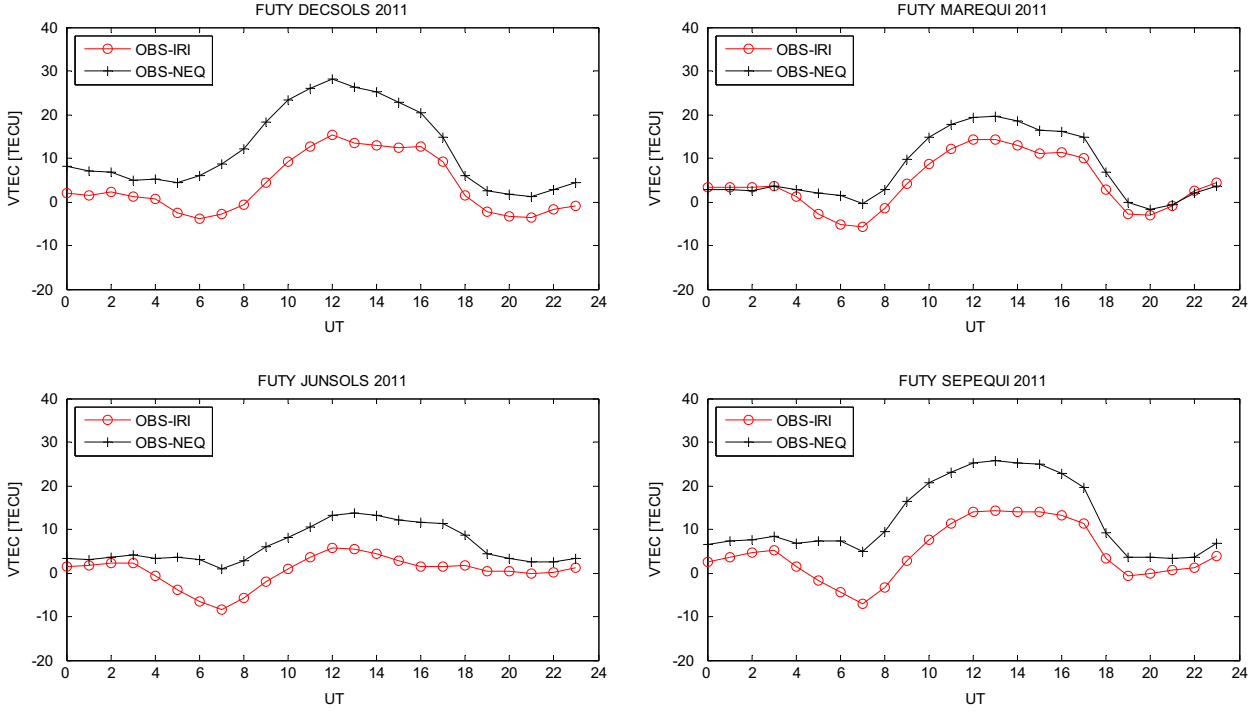

Fig. 17. Plots of $\Delta(VTEC_{OBS} - VTEC_{PRE})$ for FUTY.

50% during the night under storm-time conditions. Since the TEC for high altitude satellites includes ionospheric and plasmaspheric contributions to the total observed TEC, there is the need for adequate inclusion of the plasmaspheric contribution into the models. Generally, the predictions are relatively good in JUNSOLS for both models and worst in DECSOLS and SEPEQUI for both models, with the exception of DECSOLS in RUST. The electron concentration is largest in the equinox and this implies greatest variability in the equinox. Equatorial ionosphere experiences lower variability during JUNSOLS. Hence, the model prediction is better during periods of

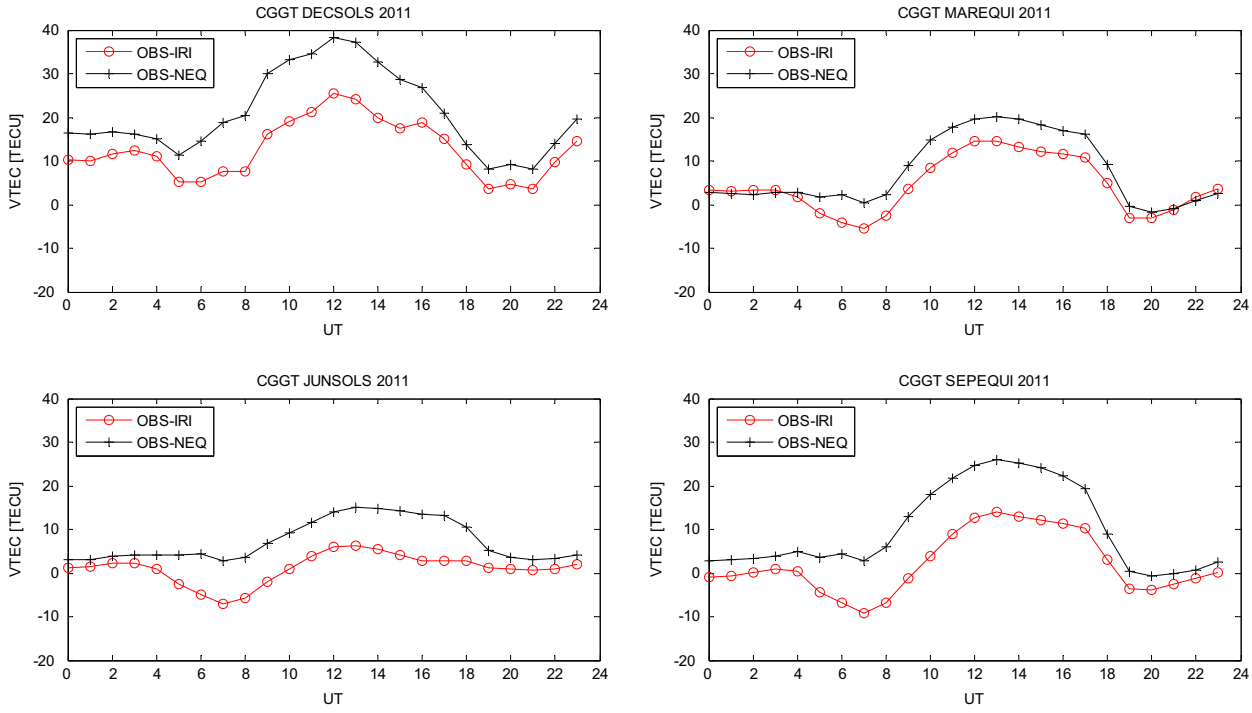

Fig. 18. Plots of $\Delta(VTEC_{OBS} - VTEC_{PRE})$ for CGGT.

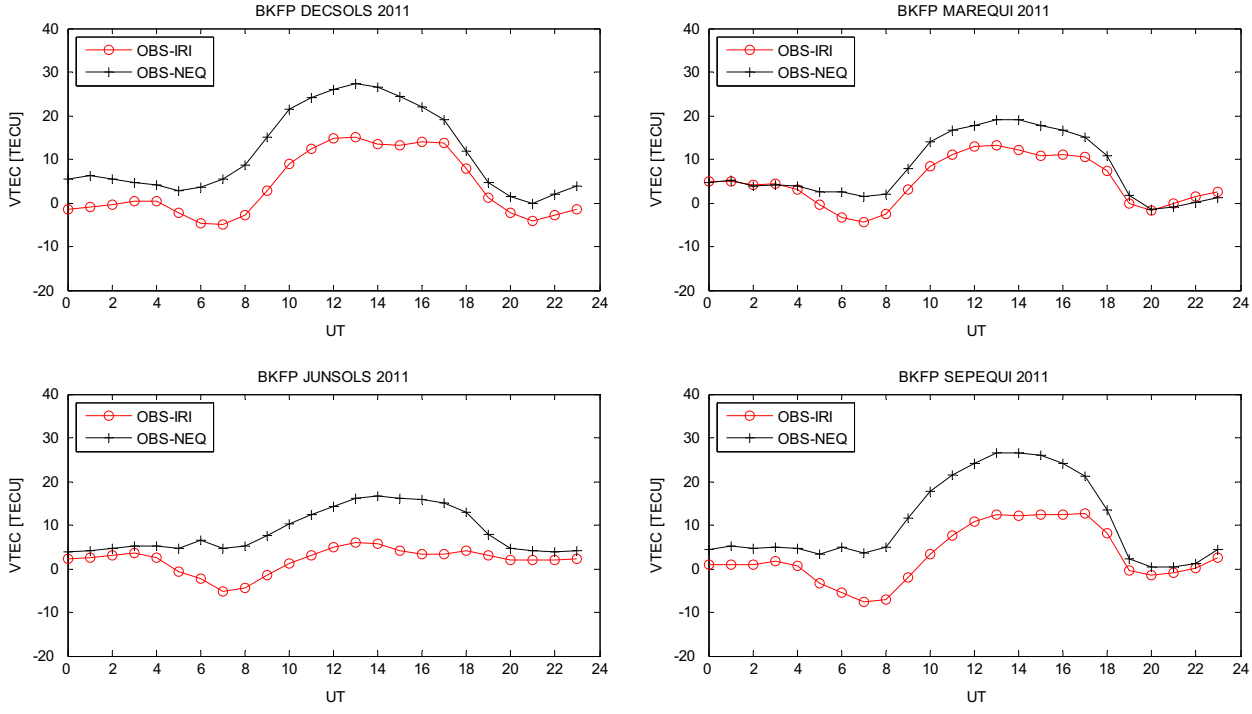

Fig. 19. Plots of $\Delta(VTEC_{OBS} - VTEC_{PRE})$ for BKFP.

lower variability. Also, the discrepancies observed may result from an inaccurate correction factor for the IRI model (Bilitza, 2004; Bilitza and Reinisch, 2008), and an inaccurate Epstein layer with a height dependent thickness (i.e. scale height) parameter, for the NeQuick model (Coïsson et al., 2006; Nava et al., 2008). The correction factor in the IRI is based on over 150,000 topside profiles from Alouette 1, 2, and ISIS 1, 2. This term varies with altitude, modified dip latitude, and local time (Bilitza, 2004).

As can be observed from Table 3, the RMSE values obtained for the two models showed that IRI2011 model performed better than NeQuick model as the IRI model

Table 3
Root mean square error for NeQuick and IRI models.

Station	RMSE for NeQuick model				RMSE for IRI model			
	DECSOLS	MAREQUI	JUNSOLS	SEPEQUI	DECSOLS	MAREQUI	JUNSOLS	SEPEQUI
RUST	3.52	10.27	5.82	4.22	9.72	8.27	3.35	5.61
UNEC	13.68	8.74	6.67	12.11	7.37	6.41	3.63	7.47
ULAG	12.82	8.72	9.82	14.14	7.06	6.19	5.31	8.63
FUTY	14.98	10.42	7.60	14.93	7.44	7.48	3.50	7.85
CGGT	22.80	10.85	8.63	13.78	14.17	7.56	3.54	7.18
BKFP	14.84	10.50	9.80	14.42	8.13	7.17	3.42	7.04

RMSE is smaller than that of the NeQuick model in all cases, except at RUST during DECSOLS and SEPEQUI.

4. Conclusion

In this study, the diurnal and seasonal variations of VTEC over Nigeria have been reported, using data from six GPS receivers. The results showed that VTEC has higher values during daytime when compared with nighttime values. TEC values generally increase from 0600 h LT in all the seasons and reach its maximum value during 1500 h–1700 h LT. Generally, the results obtained revealed that daytime values of VTEC are greater in DECSOLS while the lowest values are observed during JUNSOLS.

It can be seen that the IRI and NeQuick modelled values follow the diurnal and seasonal variation patterns of the observed values of VTEC. From the result of the RMSE, IRI model produced the best results at all locations, except at RUST during DECSOLS and SEPEQUI. More efforts need to be concentrated on increasing the upper boundary in the models to 20,000 km, in order to include the plasmaspheric TEC in the predictions. The correction factor for the IRI model and the scale height parameter for the NeQuick model can be improved upon. These suggestions are likely to improve the prediction of these models.

Acknowledgements

The GPS data used for this research were obtained from the public archives of the Office of the Surveyor General of the Federal Government of Nigeria, which is the mapping agency of Nigeria. We are also thankful to the Aeronomy and Radiopropagation Laboratory of the Abdus Salam International Centre for Theoretical Physics Trieste, Italy for allowing access to NeQuick package. We acknowledge Dieter Bilitza and the IRI team for making the IRI model available.

References

Adewale, A.O., Oyeyemi, E.O., Adeniyi, J.O., Adeloye, A.B., Oladipo, O.A., 2011. Comparison of total electron content predicted using the IRI-2007 model with GPS observations over Lagos, Nigeria. Indian J. Radio Space Phys. 40, 21–25.

Adewale, A.O., Oyeyemi, E.O., Cilliers, P.J., McKinnell, L.A., Adeloye, A.B., 2012. Low solar activity variability and IRI 2007 predictability of equatorial Africa GPS TEC. Adv. Space Res. 49, 316–326.

Aggarwal, M., 2011. TEC variability near northern EIA crest and comparison with IRI model. Adv. Space Res. 48 (7), 1221. http://dx.doi.org/10.1016/j.asr.2011.05.037.

Appleton, E.V., 1946. Two anomalies in the ionosphere. Nature 157, 691–693.

Bagiya, M.S., Joshi, H.P., Iyer, K.N., Aggarwal, M., Ravindran, S., Pathan, B.M., 2009. TEC variations during low solar activity period (2005–2007) near the equatorial ionospheric anomaly crest region in India. Ann. Geophys. 27, 1047–1057.

Balan, N., Batista, I.S., Abdu, M.A., Bailey, G.J., Watanabe, S., MacDougall, J., Sobral, J.H.A., 2000. Variability of additional layer in the equatorial ionosphere over Fortaleza. J. Geophys. Res. 105, 10603–10613.

Bhuyan, P.K., Borah, R.R., 2007. TEC derived from GPS network in India and comparison with the IRI. Adv. Space Res. 39, 830–840.

Bidaine, B., Warnant, R., 2010. Assessment of the NeQuick model at mid-latitudes using GNSS TEC and ionosonde data. Adv. Space Res. 45, 1122–1128.

Bilitza, D., 2004. A correction for the IRI topside electron density model based on Alouette/ISIS topside sounder data. Adv. Space Res. 33 (6), 838–843.

Bilitza, D., Reinisch, B.W., 2008. International reference ionosphere 2007: improvements and new parameters. Adv. Space Res. 42, 599–609.

Coïsson, P., Radicella, S.M., Leitinger, R., Nava, B., 2006. Topside electron density in IRI and NeQuick: features and limitations. Adv. Space Res. 37, 937–942.

Coïsson, P., Radicella, S.M., Nava, B., Leitinger, R., 2008. Low and equatorial latitudes topside in NeQuick. J. Atmos. Sol. Terr. Phys. 70, 901–906.

Di Giovanni, G., Radicella, S.M., 1990. An analytical model of the electron density profile in the ionosphere. Adv. Space Res. 10, 27–30.

Fejer, B.G., Farley, D.T., Gonzales, C.A., Woodman, R.F., Calderon, C., 1981. F-region east–west drifts at Jicamarca. J. Geophys. Res. 86, 215.

Gulyaeva, T.L., Gallagher, D.L., 2007. Comparison of two IRI electron-density plasmasphere extensions with GPS-TEC observations. Adv. Space Res. 39, 744–749.

Jatau, B., Fernandes, R.M.S., Adebomehin, A., Gonçalves, N., 2010. NIGNET – the new permanent GNSS network of Nigeria. In: Proceedings of the FIG Congress 2010, April 11–16, 2010, Sydney, Australia.

Kintner, P.M., Ledvina, B.M., 2005. The ionosphere, radio navigation, and global navigation satellite systems. Adv. Space Res. 35, 788–811.

Mannucci, A.J., Wilson, B.D., Edwards, C.D., 1993. A new method for monitoring the earth's ionosphere total electron content using the GPS global network, Proceedings of ION GPS-93. Institute of Navigation, pp. 1323–1332.

Migoya Orué, Y.O., Radicella, S.M., Coïsson, P., Ezquer, R.G., Nava, B., 2008. Comparing TOPEX TEC measurements with IRI predictions. Adv. Space Res. 42, 757–762.

Misra, P., Enge, P., 2006. GPS measurements and error sources, global positioning system: signals, measurements, and performance. In: Gao, G., Walter, F. (Eds.). Ganga-Jamuna Press, USA, pp. 185–194.

Mitra, S.K., 1946. Geomagnetic control of region F2 of the ionosphere. Nature 158, 608–669.

Mukherjee, S., Sarkar, S., Purohit, P.K., Gwal, A.K., 2010. Seasonal variation of total electron content at crest of equatorial anomaly station during low solar activity conditions. Adv. Space Res. 46 (3), 291–295.

Nava, B., Coïsson, P., Radicella, S.M., 2008. A new version of the NeQuick ionosphere electron density model. J. Atmos. Sol. Terr. Phys. 70, 1856–1862.

Obrou, O.K., Mene, M.N., Kobea, A.T., Zaka, K.Z., 2009. Equatorial total electron content (TEC) at low and high solar activity. Adv. Space Res. 43 (11), 1757–1761.

Okoh, D., Eze, A., Adedoja, O., Okere, B., Okeke, P.N., 2012. A comparison of IRI-TEC predictions with GPS-TEC measurements over Nsukka, Nigeria. Space Weather 10, S10002. http://dx.doi.org/10.1029/2012SW000830.

Radicella, S.M., Zhang, M.L., 1995. The improved DGR analytical model of electron density height profile and total electron content in the ionosphere. Ann. Geofis. XXXVIII (1), 35–41.

Warnant, R., Pottiaux, E., 2000. The increase of the ionospheric activity as measured by GPS. Earth Planets Space 52, 1055–1060.